Sterically Encumbered, Charge-Compensated Metallacarboranes.† Synthesis and Structures of Ruthenium Pentamethylcyclopentadienyl Derivatives

Georgina M. Rosair, Alan J. Welch,* and Andrew S. Weller

Department of Chemistry, Heriot-Watt University, Edinburgh EH14 4AS, U.K.

Received May 6, 1998

The reactions of $[RuCl(Cp^*)]_4$ with monoanionic, charge-compensated carborane anions have been studied and products characterized by NMR spectroscopy (^1H and ^{11}B) and single-crystal *X*-ray diffraction. With $[9\text{-}SMe_2\text{-}7,8\text{-}nido\text{-}C_2B_9H_{10}]^-$, the product is the expected species 3-(Cp*)-4-SMe_2-3,1,2-*closo*-$RuC_2B_9H_{10}$, the structure of which reveals some evidence for steric congestion between the Cp* and SMe_2 substituents, which is characteristic of all of the compounds studied. Use of the carborane anion $[7\text{-}Ph\text{-}9\text{-}SMe_2\text{-}7,8\text{-}nido\text{-}C_2B_9H_9]^-$ affords 1-Ph-3-(Cp*)-7-SMe_2-3,1,2-*closo*-$RuC_2B_9H_9$, in which the Ph and SMe_2 cage substituents are separated by a {BH} unit. ^1H NMR spectroscopy of this compound reveals restricted rotation of the phenyl group at room temperature. Moreover, the compound isomerizes, slowly at room temperature but rapidly if warmed, to the C_{cage}-separated isomer 3-(Cp*)-4-SMe_2-11-Ph-3,1,2-*closo*-$RuC_2B_9H_9$. In contrast, and somewhat surprisingly, the analogous compound 1-Ph-3-(Cp*)-4-SMe_2-3,1,2-*closo*-$RuC_2B_9H_9$ (prepared from $[RuCl(Cp^*)]_4$ and $[7\text{-}Ph\text{-}11\text{-}SMe_2\text{-}7,8\text{-}nido\text{-}C_2B_9H_9]^-$), which has adjacent Ph and SMe_2 substituents, does not isomerize, even when heated. The reaction between $[RuCl(Cp^*)]_4$ and $[7,8\text{-}Ph_2\text{-}9\text{-}SMe_2\text{-}7,8\text{-}nido\text{-}C_2B_9H_8]^-$ affords 1,2-Ph_2-3-(Cp*)-4-SMe_2-3,1,2-*pseudocloso*-$RuC_2B_9H_8$, the first example of a charge-compensated pseudocloso metallacarborane.

Introduction

We have previously reported the stereochemical consequences of deliberate overcrowding in metallacarboranes based upon the $[7,8\text{-}Ph_2\text{-}7,8\text{-}nido\text{-}C_2B_9H_9]^{2-}$ ligand. Such overcrowding can result in deviations from conventional polytopal architectures[2] (*pseudocloso* structures) or lead to low-temperature polytopal isomerizations,[3] and in one instance has allowed the first isolation of an intermediate on such an isomerization pathway.[4]

To extend this chemistry further to incorporate cage systems other than the ubiquitous $[7\text{-}R\text{-}8\text{-}R'\text{-}7,8\text{-}nido\text{-}C_2B_9H_9]^{2-}$ ligand (R, R′ = H, Me, Ph), we have recently described the synthesis and characterization of sterically crowded derivatives of the charge-compensated carborane 9-SMe_2-7,8-*nido*-$C_2B_9H_{11}$ (compound **I**, Chart 1), which afford monoanionic fragments on deprotonation.[5] In these systems (**II** and **III**), we found that the only isolatable product of the reaction between nido anions and $[RhCl(CO)_2]_2$ was 1-Ph-3,3-$(CO)_2$-7-SMe_2-3,1,2-*closo*-$RhC_2B_9H_9$, compound **IV**, following deprotonation of **IIa**. We rationalized this behavior in terms of the electronically preferred conformation of the $\{Rh(CO)_2\}$ fragment, which was attainable in **IV** but could not be supported in analogous complexes formed from **IIb** or **III** due to steric pressure from the adjacent SMe_2 and Ph groups.

Chart 1

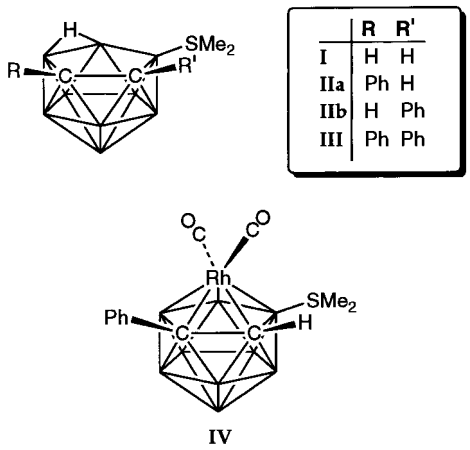

IV

In the anticipation that addition of a suitable capping metal−ligand fragment to deprotonated **IIb** or **III** would possibly lead to polytopal deformations or isomerizations, similar to those observed with $[7,8\text{-}Ph_2\text{-}7,8\text{-}nido\text{-}C_2B_9H_9]^{2-}$, a metal−ligand fragment more robust than $\{Rh(CO)_2\}$ was sought.

† Part 18 of the series "Steric Effects in Heteroboranes". For part 17 see ref 1.

(1) Welch, A. J.; Weller, A. S. *J. Chem. Soc., Dalton Trans.* **1997**, 1205.
(2) For a recent example and leading references, see: Thomas, Rh. Ll.; Welch, A. J. *J. Chem. Soc., Dalton Trans.* **1997**, 631.
(3) Baghurst, D. R.; Copley, R. C. B.; Fleischer, H.; Mingos, D. M. P.; Kyd, G. O.; Yellowlees, L. J.; Welch, A. J.; Spalding, T. R.; O'Connell, D. *J. Organomet. Chem.* **1993**, *447*, C14.
(4) Dunn, S.; Rosair, G. M.; Thomas, Rh. Ll.; Weller, A. S.; Welch, A. J. *Angew. Chem., Int. Ed. Engl.* **1997**, *36*, 645.
(5) Rosair, G. M.; Welch, A. J.; Weller, A. S.; Zahn, S. K. *J. Organomet. Chem.* **1997**, *536*, 299.

S0276-7333(98)00353-7 CCC: $15.00
Publication on Web 06/25/1998

We report here the synthesis and structural characterization of new metallacarborane complexes formed between deprotonated **I**, **IIa**, **IIb**, and **III** and $\{Ru(Cp^*)\}^+$, the latter having recently been shown to be a versatile synthon in metal-cluster build up reactions.[6] We also report the characterization of derivatives resulting from the relief of steric overcrowding present in some of these systems.

Experimental Section

General Comments. All experiments were carried out under a dry, oxygen-free dinitrogen atmosphere with the new compounds reported being stable as solids at ambient atmosphere and only slightly sensitive as solutions. All solvents were stored over the appropriate drying agents and distilled immediately prior to use: CH_2Cl_2 and THF; CaH_2, 40−60 °C light petroleum fractions; Na wire, diethyl ether; Na wire/benzophenone ketyl. Microanalyses were performed by the departmental service. Chromatography columns (3 × 15 cm) were packed with silica (Kieselgel 60, 200−400 mesh). Preparative thin-layer chromatography (TLC) was performed using glass plates coated with Kieselgel 60 F_{254} (0.2 mm thick), prewashed with pure eluant. The compounds 9-SMe_2-7,8-*nido*-$C_2B_9H_{11}$ (**I**),[7] 7-Ph-9-SMe_2-7,8-*nido*-$C_2B_9H_{10}$ (**IIa**),[5] and 7-Ph-11-SMe_2-7,8-*nido*-$C_2B_9H_{10}$ (**IIb**)[5] were prepared as described previously. 7,8-Ph_2-9-SMe_2-7,8-*nido*-$C_2B_9H_9$ (**III**) was prepared by a slight modification to the previously published procedure[5] (see below). The compound $[RuCl(Cp^*)]_4$ was prepared according to the literature.[8]

NMR Spectroscopy. ^{1}H NMR spectra were recorded on Bruker AC200 and DPX400 spectrometers. ^{11}B and variable-temperature ^{1}H NMR spectra were recorded on the DPX400 spectrometer. Unless otherwise stated, measurements were made at 297 K from $CDCl_3$ solutions. Proton chemical shifts are reported relative to residual protio solvent in the sample, and ^{11}B shifts (at 128.4 MHz) are reported relative to external $BF_3{\cdot}OEt_2$.

7,8-Ph_2-9-SMe_2-7,8-*nido*-$C_2B_9H_9$ (III), Modified Procedure.[5] K[7,8-Ph_2-7,8-*nido*-$C_2B_9H_{10}$] (2.20 g, 6.8 mmol) was dissolved in H_2O (2 cm^3) and DMSO (9 cm^3) and cooled to 0 °C. H_2SO_4 (concentrated, 18 cm^3) was added dropwise to the solution over 15 min, and the resulting off-white suspension was stirred at room temperature for 3 days. H_2O (30 cm^3) was added, and the white precipitate was filtered off and washed with water (3 × 20 cm^3). The solid was dissolved in CH_2Cl_2 (40 cm^3) and dried over $MgSO_4$. Removal of solvent and recrystallization from CH_2Cl_2/light petroleum afforded 7,8-Ph_2-9-SMe_2-7,8-*nido*-$C_2B_9H_9$, compound **III**, mass 1.30 g, yield 71%, as a white powder. ^{1}H and ^{11}B NMR spectroscopy confirmed the identity and purity of **III**.

3-(Cp*)-4-SMe_2-3,1,2-*closo*-$RuC_2B_9H_{10}$, 1. 9-SMe_2-7,8-*nido*-$C_2B_9H_{11}$, **I**, (0.100 g, 0.52 mmol) was added to a THF (25 cm^3) suspension of prewashed NaH (0.040 g, excess). The solution was heated to reflux for 45 min and allowed to settle. The supernatant was carefully removed via syringe and added to a frozen (liquid nitrogen) solution of $[RuCl(Cp^*)]_4$ (0.142 g, 0.13 mmol) in THF (10 cm^3). The mixture was warmed slowly to room temperature and stirred for a further 18 h. The solvent was removed in vacuo, and the residue was dissolved in CH_2Cl_2 and filtered through a Celite plug. The solvent was reduced in volume to ca. 2 cm^3 and applied to the top of a chromatography column. Elution with CH_2Cl_2 afforded a single yellow band, which was collected and recrystallized from CH_2Cl_2/light petroleum to afford 0.12 g (54%) of 3-(Cp*)-4-SMe_2-3,1,2-*closo*-$RuC_2B_9H_{10}$, **1**, as very pale yellow microcrystals. Anal. Calcd for $C_{14}H_{31}B_9RuS$: C, 39.1; H, 7.29. Found: C, 39.5; H, 7.40.

^{1}H NMR δ/ppm: 3.32 (br, 1H, C_{cage}−H), 2.67 (br, 1H, C_{cage}−H), 2.54 (s, 3H, SMe), 2.39 (s, 3H, SMe), 1.88 (s, 15 H, C_5Me_5). ^{11}B{^{1}H} NMR δ/ppm: −0.40 (1B), −3.09 (1B), −4.44 (1B), −6.35 (1B), −11.49 (1B), −15.82 (1B), −21.87 (1B), −23.75 (1B), −25.90 (1B).

1-Ph-3-(Cp*)-7-SMe_2-3,1,2-*closo*-$RuC_2B_9H_9$, 2. Similarly, 7-Ph-9-SMe_2-7,8-*nido*-$C_2B_9H_{10}$, **IIa** (0.075 g, 0.28 mmol), in THF (20 cm^3) was deprotonated and reacted with $[RuCl(Cp^*)]_4$ (0.075 g, 0.07 mmol) in THF (10 cm^3). Chromatography eluting with CH_2Cl_2:light petroleum (3:2) afforded a minor pale yellow band followed closely by a major orange band, both of which were collected. The major product was recrystallized from CH_2Cl_2/light petroleum to afford 0.080 g (56%) of 1-Ph-3-(Cp*)-7-SMe_2-3,1,2-*closo*-$RuC_2B_9H_9$, **2**, as yellow plates. The minor product was subsequently identified as compound **3**. Anal. Calcd for $C_{20}H_{35}B_9RuS$: C, 47.5; H, 6.97. Found: C, 47.6; H, 6.72.

^{1}H NMR (−60 °C) δ/ppm: 7.10 (m, 2H, Ph_{meta}), 6.92 (m, 1H, Ph_{para}), 6.85 (d, 1H, Ph_{ortho}, J(HH) 9 Hz), 6.56 (d, 1H, Ph_{ortho}, J(HH) 9 Hz), 3.95 (s br, 1H, C_{cage}−H), 2.40 (s, 3H, SMe), 2.35 (s, 3H, SMe), 1.38 (s, 15H, C_5Me_5). ^{11}B{^{1}H} NMR δ/ppm: 1.58 (2B, 1 + 1 coincidence), −3.10 (2B, 1 + 1 coincidence), −4.23 (1B), −11.37 (1B), −15.93 (1B), −19.43 (1B), −22.94 (1B).

3-(Cp*)-4-SMe_2-11-Ph-3,1,2-*closo*-$RuC_2B_9H_9$, 3. A sample of complex **2** (0.045 g, 0.09 mmol) was kept at room temperature as a $CDCl_3$ solution for 5 days, until only peaks due to a new complex were present in the ^{1}H NMR spectrum. Layering the solvent with 60−80 °C light petroleum and cooling to −30 °C for 5 days afforded 0.041 g (92%) of 3-(Cp*)-4-SMe_2-11-Ph-3,1,2-*closo*-$RuC_2B_9H_9$, **3**, as pale yellow diffraction-quality crystals. Alternatively complex **3** may be prepared by heating to reflux a $CHCl_3$ solution of **2** for 4 h. Anal. Calcd for $C_{20}H_{35}B_9RuS$: C, 47.5; H, 6.97. Found: C, 47.0: H, 6.52.

^{1}H NMR δ/ppm: 7.46 (m, 2H, Ph), 7.07(m, 3H, Ph), 2.54 (s, 3H, SMe), 2.47 (s, 3H, SMe), 2.12 (s br, 1H, C_{cage}−H), 1.40 (s, 15H, C_5Me_5). ^{11}B{^{1}H} NMR δ/ppm: 1.27 (2B, 1 + 1 coincidence), −4.00 (sh, 1B), −5.92 (1B), −6.80 (sh, 1B), −10.90 (1B), −21.42 (1B), −22.63 (1B), −23.69 (1B).

1-Ph-3-(Cp*)-4-SMe_2-3,1,2-*closo*-$RuC_2B_9H_9$, 4. In conditions similar to those employed for the synthesis of compound **1**, 7-Ph-11-SMe_2-7,8-*nido*-$C_2B_9H_{10}$, **IIb** (0.075 g, 0.28 mmol), was deprotonated with NaH and reacted with $[RuCl(Cp^*)]_4$ (0.075 g, 0.07 mmol). Column chromatography (CH_2Cl_2:light petroleum = 9:1) afforded a fast moving minor band (identified as free ligand) and a major orange band, which was recrystallized from CH_2Cl_2/petroleum ether to afford 0.065 g (46%) of 1-Ph-3-(Cp*)-4-SMe_2-3,1,2-*closo*-$RuC_2B_9H_9$, **4**, as pale yellow microcrystals. Anal. Calcd for $C_{20}H_{35}B_9RuS$: C, 47.5; H, 6.97. Found: C, 48.0; H, 7.32.

^{1}H NMR δ/ppm: 7.12 (m, 2H, Ph), 6.93 (m, 1H, Ph), 6.52 (m, 2H, Ph), 3.18 (s br, 1H, C_{cage}−H), 2.54 (s, 3H, SMe), 2.48 (s, 3H, SMe), 1.43 (s, 15H, C_5Me_5). ^{11}B{^{1}H} NMR δ/ppm: 0.84 (1B), 0.05 (sh, 1B), −4.50 (2B, 1 + 1 coincidence), −11.19 (1B), −15.47 (1B), −19.08 (2B, 1 + 1 coincidence), −20.27 (1B).

1,2-Ph_2-3-(Cp*)-4-SMe_2-3,1,2-*pseudocloso*-$RuC_2B_9H_8$, 5. Similarly, 7,8-Ph_2-9-SMe_2-7,8-*nido*-$C_2B_9H_9$, **III**, (0.130 g, 0.38 mmol) was deprotonated with NaH and reacted with $[RuCl(Cp^*)]_4$ (0.100 g, 0.09 mmol) overnight. The solvent was removed in vacuo, and the residue was dissolved in CH_2Cl_2 (2 cm^3) and applied to a preparative TLC plate. Elution with CH_2Cl_2:light petroleum (1:1) afforded a pale yellow band ($R_f \approx 0.6$, free ligand) and a slower moving brown band ($R_f \approx 0.35$), which was recovered and recrystallized from CH_2Cl_2/light petroleum to afford brown microcrystals of 1,2-Ph_2-3-(Cp*)-4-SMe_2-3,1,2-*pseudocloso*-$RuC_2B_9H_8$, mass 0.025 g (yield 12%). Anal. Calcd for $C_{26}H_{40}B_9RuS$: C, 53.6; H, 6.92. Found: C, 53.9; H 7.21.

(6) Lewis, J.; Morewood, C. A.; Raithby, P. R.; Ramirez de Arellano, M. C. *J. Chem. Soc., Dalton Trans.* **1996**, 4509.

(7) Plesek, J.; Janousek, Z.; Hermanek, S. *Collect. Czech. Chem. Commun.* **1978**, *43*, 2862.

(8) Fagan, P. J.; Ward, M. D.; Calabrese, J. C. *J. Am. Chem. Soc.* **1989**, *111*, 1698.

Table 1. Crystallographic Data for Compounds 1−5

	1	2	3	4	5
formula	$C_{14}H_{31}B_9RuS$	$C_{23}H_{42}B_9ClRuS$	$C_{20}H_{35}B_9RuS$	$C_{20}H_{35}B_9RuS$	$C_{26}H_{39}B_9RuS$
mol wt	429.81	584.44	505.90	505.90	581.99
cryst syst	monoclinic	orthorhombic	monoclinic	orthorhombic	monoclinic
space group	$P2_1/c$	$Pca2_1$	$P2_1$	$P2_12_12_1$	$P2_1/c$
a (Å)	14.063(2)	13.125(2)	9.382(2)	8.6389(6)	10.452(2)
b (Å)	8.732(2)	26.458(3)	13.719(3)	16.6560(10)	15.732(2)
c (Å)	18.131(3)	16.491(2)	10.422(2)	17.2269(10)	17.097(2)
β (deg)	111.997(14)	90	111.499(9)	90	97.855(10)
V (Å^3)	2064.3(7)	5726.7(13)	1248.1(4)	2478.8(3)	2785.0(6)
Z	4	8	2	4	4
cryst dimens (mm)	0.1 × 0.2 × 0.8	0.8 × 0.4 × 0.1	0.05 × 0.3 × 0.5	0.2 × 0.2 × 0.3	0.3 × 0.2 × 0.2
D_{calc} (g cm^{-3})	1.383	1.356	1.346	1.356	1.388
μ(Mo Kα) (mm^{-1})	0.855	0.726	0.718	0.723	0.654
F(000) (e)	880	2416	520	1040	1200
2θ range (deg)	3−50	3−50	5−50	3−50	3−50
hkl range	−1 to 16; −1 to 10; −21 to 20	−1 to 15; −31 to 1; −1 to 19	−1 to 11; −1 to 16; −12 to 11	−1 to 7; −1 to 19; −1 to 20	−1 to 12; −1 to 18; −20 to 20
no. of unique data collected	3611	5576	2356	2734	4867
no. data used in refinement	3610	5573	2356	2733	4866
wR^2 (R with $I > 2\sigma(I)$)[a]	0.0825 (0.0389)	0.1286 (0.0537)	0.1008 (0.0437)	0.0781 (0.0346)	0.0971 (0.0610)
S	1.049	1.060	1.041	0.935	1.003
a, b	0.0354, 0.06626	0.0786, 2.56	0.0607, 0	0.0456, 1.48	0.0256, 0
max/min residue (e Å^{-3})	+ 0.515/−0.577	+ 0.718/−0.501	+ 0.967/−0.717	+ 0.291/−0.339	+ 0.497/−0.447

[a] $R = \Sigma||F_o| - |F_c||/\Sigma|F_o|$; w$R^2 = [\Sigma[w(F_o^2 - F_c^2)^2]/\Sigma[w(F_o^2)^2]]^{1/2}$, $S = [\Sigma[w(F_o^2 - F_c^2)^2]/(n - p)]^{1/2}$ (n = no. data, p = no. variables).

^{1}H NMR δ/ppm: 7.40−6.81 (m, 10H, Ph), 2.53 (s, 3H, SMe), 2.08 (s, 3H, SMe). ^{11}B{^{1}H} NMR δ/ppm: 27.21 (1B), 14.68 (1B), 8.79 (1B), 2.75 (1B), −1.63 (1B), −2.68 (2B, 1 + 1 coincidence), −6.30 (1B), −16.40 (1B).

X-ray Crystallography. Measurements on compounds **1**−**5** were carried out at room temperature using a Siemens P4 diffractometer equipped with graphite-monochromated Mo Kα *X*-radiation (λ = 0.710 69 Å). Data collection (ω scans) and reduction were under the control of XSCANS.[9] Structure solution and refinement were performed using the SHELXTL system[10] on a Pentium 90 MHz PC. Table 1 lists details of unit cell data, intensity data collection and structure refinement. The unit cell parameters and orientation matrix for data collection, were determined by the least squares-refinement of the setting angles of 26, 26, 36, 42, and 26 centered reflections, respectively, with 2θ ranging from 9° to 25°. Standard reflections were remeasured every 100 data; some crystal decay was found (6.5−13.4%) for which correction was applied. Data were corrected for absorption by ψ scans. All structures were solved by direct and difference Fourier methods and refined by full-matrix least-squares against F^2. Cage C atoms without a bound phenyl substituent (compounds **1**−**4**) were identified by low U_{iso} values and short C−C or C−B distances following refinement as B. Crystals of compound **2** contained one partially disordered CH_2Cl_2 molecule and one rather ill-defined pentane molecule of solvation per two molecules of metallacarborane. The first was modeled using two 0.7 occupancy Cl positions and two 0.3 occupancy Cl positions, with C−Cl distances restrained to 1.70(5) Å. In the pentane molecule, C−C distances were restrained to 1.50(5) Å. No hydrogen atoms were included in either solvent model.

All phenyl and methyl H atoms were set in calculated positions riding on the bound C atom with U_{iso} 1.2 and 1.5 times the bound carbon atom U_{eq}, respectively. Terminal cage B-bonded H atom positions were similarly treated (U_{iso} 1.2 times the boron atom U_{eq}), but cage C-bonded H atoms were located in the difference map and refined subject to the C−H distance being restrained to 1.15 Å. Data were weighted such that $w^{-1} = [\sigma^2(F_o)^2 + (aP)^2 + bP]$, where $P = [0.333 \max(F_o^2 \text{ or } 0) + 0.667F_c^2]$.

(9) *XSCANS*; Siemens Analytical Instruments, Inc.: Madison, WI, 1994.

(10) Sheldrick, G. M. *SHELXTL/PC*; Siemens Analytical Instruments, Inc.: Madison, WI, 1994.

Results and Discussion

Reaction between $[RuCl(Cp^*)]_4$ and 1 mol equiv of Na[9-SMe_2-7,8-*nido*-$C_2B_9H_{10}$] (formed by deprotonation of **I** with NaH) resulted in the isolation, in reasonable yield after column chromatography, of the new charge-compensated ruthenacarborane 3-(Cp^*)-4-SMe_2-3,1,2-*closo*-$RuC_2B_9H_{10}$, **1**. Compound **1** was initially characterized by ^{1}H and ^{11}B NMR spectroscopy. In the ^{1}H NMR spectrum, the cage C−H atoms resonate at 3.32 and 2.67 ppm and the signals due to the magnetically inequivalent S−Me protons appear at 2.54 and 2.39 ppm. The ^{11}B{^{1}H} NMR spectrum reveals nine resonances of approximately equal intensity between −0.4 and −25.9 ppm, with that at −3.09 ppm remaining a singlet on retention of proton coupling and thus assigned to B(4). The weighted average ^{11}B chemical shift, $<\delta(^{11}B)>$, is −12.57 ppm, indicative of a *closo*-MC_2B_9 metallacarborane.[2]

As **1** constituted the first (and sterically least crowded) member of this series of ruthenacarboranes, its solid-state structure was determined by a single-crystal *X*-ray diffraction study. The molecular structure of **1**, demonstrating the atom-labeling scheme used, is shown in Figure 1, while selected bond lengths and angles are given in Table 2. Compound **1** has the expected *closo*-MC_2B_9 geometry and is similar in overall structure to the related cation [3-(Cp^*)-4-SMe_2-3,1,2-$FeC_2B_9H_{10}$]$^+$.[11] Notably, C(1)−C(2) is 1.642(6) Å and C(1)−B(4) is 1.712(6) Å, the latter being comparable with other C−B lengths. The ruthenium atom is located 1.608 Å above the mean plane defined by C(1), C(2), B(4), B(7), and B(8). Ru−B distances are similar to those found in other *closo*-RuC_2B_9 mixed-sandwich systems,[12,13] with Ru(3)−B(8) 2.231(5) Å being slightly the longest.

(11) Yan, Y.-K.; Mingos, D. M. P.; Müller, T. E.; Williams, D. J.; Kurmoo, M. *J. Chem. Soc., Dalton Trans.* **1995**, 2509.

(12) Kennedy, J. D. *Prog. Inorg. Chem.* **1986**, *34*, 211.

(13) (a) Fontaine, X. L. R.; Greenwood, N. N.; Kennedy, J. D.; Plesek, J.; Stibr, B.; Thornton-Pett, M. *Acta Crystallogr., Sect. C* **1990**, *46*, 995. (b) Cowie, J.; Reid, B. D.; Watmough, J. M. S.; Welch, A. J. *J. Organomet. Chem.* **1994**, *481*, 283.

Table 2. Selected Bond Lengths (Å) and Angles (deg) in Compound 1

Ru(3)−B(4)	2.174(5)	Ru(3)−C(34)	2.184(4)	Ru(3)−C(35)	2.189(4)
Ru(3)−C(33)	2.194(4)	Ru(3)−B(7)	2.197(6)	Ru(3)−C(32)	2.208(5)
Ru(3)−C(31)	2.224(5)	Ru(3)−B(8)	2.231(5)	S(1)−C(21)	1.795(5)
S(1)−C(20)	1.796(5)	S(1)−B(4)	1.907(5)	C(1)−C(2)	1.642(6)
C(1)−B(4)	1.712(6)	C(1)−B(5)	1.724(6)	C(1)−B(6)	1.732(7)
C(1)−Ru(3)	2.162(4)	C(2)−B(11)	1.708(7)	C(2)−B(7)	1.732(7)
C(2)−B(6)	1.732(7)	C(2)−Ru(3)	2.144(5)	B(4)−B(9)	1.769(7)
B(4)−B(8)	1.789(7)	B(4)−B(5)	1.795(7)	B(5)−B(6)	1.748(8)
B(5)−B(10)	1.765(8)	B(5)−B(9)	1.787(7)	B(6)−B(11)	1.742(8)
B(6)−B(10)	1.757(8)	B(7)−B(12)	1.775(8)	B(7)−B(8)	1.794(8)
B(7)−B(11)	1.808(7)	B(8)−B(12)	1.793(7)	B(8)−B(9)	1.801(7)
B(9)−B(12)	1.780(8)	B(9)−B(10)	1.783(8)	B(10)−B(11)	1.766(8)
B(10)−B(12)	1.785(8)	B(11)−B(12)	1.773(8)		
C(2)−Ru(3)−C(1)	44.8(2)	C(2)−Ru(3)−B(4)	78.3(2)	C(1)−Ru(3)−B(4)	46.5(2)
C(34)−Ru(3)−C(35)	37.7(2)	C(34)−Ru(3)−C(33)	38.6(2)	C(35)−Ru(3)−C(33)	63.4(2)
C(2)−Ru(3)−B(7)	47.0(2)	C(1)−Ru(3)−B(7)	79.9(2)	B(4)−Ru(3)−B(7)	81.3(2)
C(34)−Ru(3)−C(32)	63.8(2)	C(35)−Ru(3)−C(32)	63.2(2)	C(33)−Ru(3)−C(32)	37.8(2)
C(34)−Ru(3)−C(31)	62.9(2)	C(35)−Ru(3)−C(31)	37.4(2)	C(33)−Ru(3)−C(31)	62.8(2)
B(7)−Ru(3)−C(31)	156.6(2)	C(32)−Ru(3)−C(31)	37.6(2)	C(2)−Ru(3)−B(8)	79.8(2)
C(1)−Ru(3)−B(8)	80.5(2)	B(4)−Ru(3)−B(8)	47.9(2)	C(34)−Ru(3)−B(8)	114.8(2)
C(35)−Ru(3)−B(8)	104.8(2)	C(33)−Ru(3)−B(8)	149.8(2)	B(7)−Ru(3)−B(8)	47.8(2)
C(32)−Ru(3)−B(8)	163.2(2)	C(31)−Ru(3)−B(8)	125.8(2)	C(21)−S(1)−C(20)	99.8(3)
C(21)−S(1)−B(4)	109.9(2)	C(20)−S(1)−B(4)	100.6(3)		

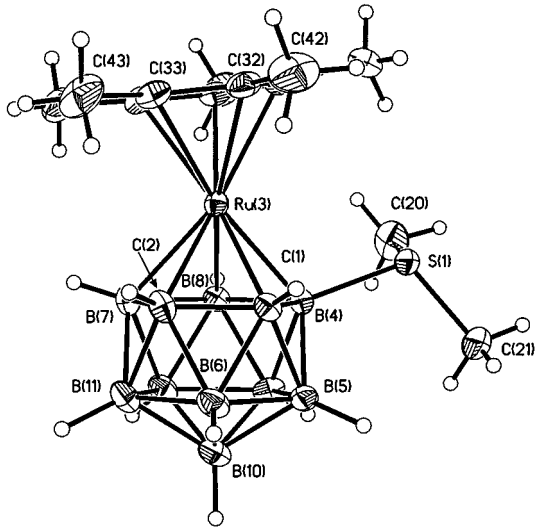

Figure 1. Perspective view of compound **1**. Thermal ellipsoids are drawn at the 40% probability level except for H atoms, which have an artificial radius for clarity.

The twist of the dimethyl sulfide substituent in 9-SMe_2-7,8-*nido*-$C_2B_9H_{11}$, its analogues, and their metal complexes has been described previously by the parameter τ[14] (the calculated torsion angle C(1)−B(4)−S(1)−S(lone pair)). In the parent carborane and its uncrowded derivatives,[14−16] τ adopts relatively small values, typically ca. −3° to −21° (the minus sign representing a clockwise rotation about the S−B bond when viewed from sulfur for the enantiomer shown in Figure 1) as the result of weak S(lone pair)···$H(1)^{\delta+}$ interaction. In the compounds reported in the present paper, we would expect τ to be influenced most strongly by the steric demands of the capping Cp* ligand. In **1**, τ is found to be −33.3° and the closest Cp*···SMe_2 H···H distance is 2.48 Å, between H(20A) and H(45A).

A further consequence of the interaction between the Cp* and SMe_2 groups is that the plane [C(31)−C(35)] of the η-bound ligand is inclined at 7.1° to the metal-bonded C_2B_3 pentagon, with Ru−C(31) significantly being the longest Ru−C(Cp*) distance. Moreover, the methyl group nearest to the SMe_2 ligand, C(41), is displaced 0.201 Å above the η-ligand plane.

Similarly, deprotonation of **IIa** and subsequent reaction with $[RuCl(Cp^*)]_4$ affords the new compound 1-Ph-3-(Cp*)-7-SMe_2-3,1,2-$RuC_2B_9H_{10}$, **2**, in fair yield after column chromatography. The $^{11}B\{^1H\}$ NMR spectrum of compound **2** is indicative of an asymmetric *closo*-MC_2B_9 cage architecture, with seven resonances observed between 1.6 and −23.0 ppm and $\langle\delta(^{11}B)\rangle$ = −8.55 ppm. One of the resonances at −3.10 ppm is assigned to B(7). As well as resonances due to Cp* and cage C−H, the room-temperature ^1H NMR spectrum displays two singlets at 2.43 and 2.48 ppm assigned to the inequivalent SMe groups. The phenyl group is observed as three signals, a sharp multiplet and a triplet at 7.16 and 6.94 ppm with an intensity of 2 and 1, respectively, and a broad, intensity 2, signal centered on 6.80 ppm. On cooling to −60 °C, this last signal decoalesces and is resolved into two doublets of equal intensity (Figure 2) while the signals arising from SMe_2, Cp*, and C−H remain essentially unchanged. A ^1H−^1H NOESY experiment (−60 °C) showed that the decoalesed peaks are due to ortho phenyl protons, the signal centered on 6.56 ppm additionally showing a strong cross-peak contact with that due to the cage C−H(2) proton. Thus, at room temperature, the phenyl ring appears to undergo restricted rotation on the NMR time scale, presumably due to steric congestion between it and the capping Cp* ligand. Similar behavior has previously been observed in the phenyl-substituted metallacarboranes 1-Ph-3-(η^5−C_9H_7)-3,1,2-*closo*-$CoC_2B_9H_{10}$[17] and 1-Ph-3-(η^5−C_9Me_7)-3,1,2-*closo*-$RhC_2B_9H_{10}$.[18]

To investigate its static molecular structure, compound **2** was studied crystallographically. The com-

(14) Cowie, J.; Hamilton, E. J. M.; Laurie, J. C. V.; Welch, A. J. *J. Organomet. Chem.* **1990**, *394*, 1.
(15) (a) Hamilton, E. J. M.; Welch, A. J. *Polyhedron* **1991**, *10*, 471. (b) Cowie, J.; Hamilton, E. J. M.; Laurie, J. C. V.; Welch, A. J. *Acta Crystallogr., Sect. C* **1988**, *44*, 1648.
(16) Douek, N. L.; Welch, A. J. *J. Chem. Soc., Dalton Trans.* **1993**, 1917.
(17) Lewis, Z. G.; Reed, D.; Welch, A. J. *J. Chem. Soc., Dalton Trans.* **1992**, 731.
(18) Grädler, U.; Weller, A. S.; Welch, A. J.; Reed, D. J. *J. Chem. Soc., Dalton Trans.* **1996**, 335.

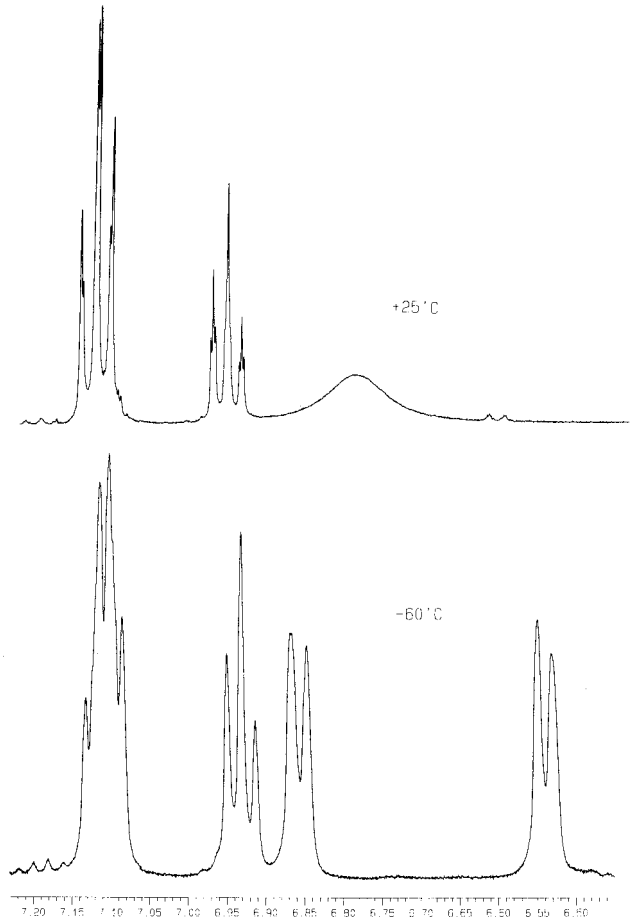

Figure 2. The aromatic region of the ^{1}H NMR spectrum of compound **2** at 25 and at −60 °C.

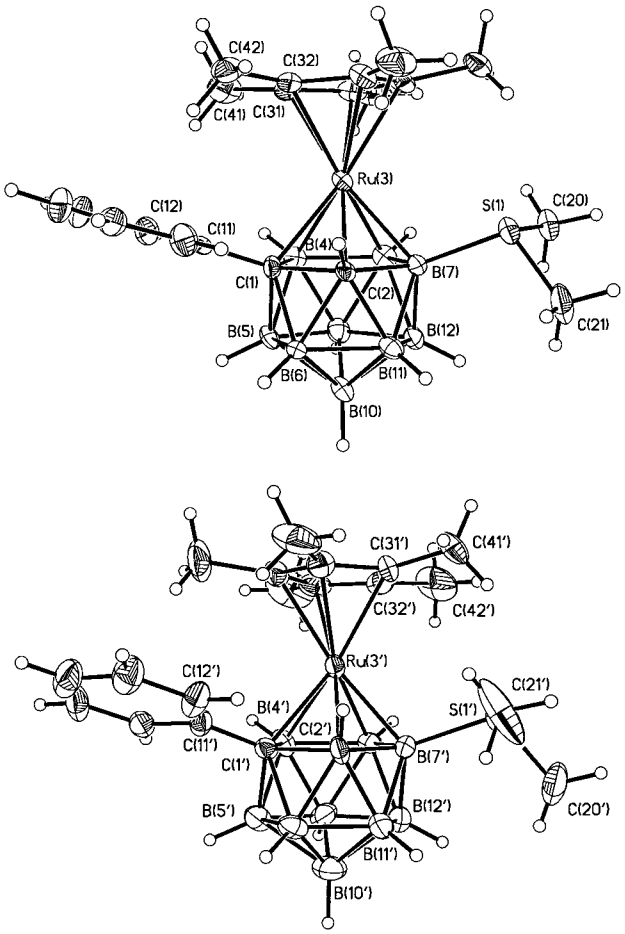

Figure 3. Perspective views of both crystallographically independent molecules of compound **2**, with thermal ellipsoids and H atoms drawn as in Figure 1.

pound crystallizes with two independent molecules (**2** and **2′**) in the asymmetric fraction of the unit cell, and perspective views of both molecules are given in Figure 3. Table 3 gives the pertinent molecular parameters. The major difference between molecules **2** and **2′** in the solid state is the orientation of the SMe_2 ligand. For **2**, τ is −43.8°, while in **2′**, τ is 66.6° (note the difference in sign). Thus, in molecule **2** the sulfur lone pair is on the same side of the cluster as the cage C−H unit, the conformation adopted in all of the other complexes and derivatives of 9-SMe_2-7,8-*nido*-$C_2B_9H_{11}$ studied crystallographically to date, while in molecule **2′** it is on the opposite side. It appears that the conformation of the SMe_2 unit in solution at −60 °C approximates that displayed by molecule **2′** in the solid state in that a cross-peak is observed between H(2) and only *one* of the S-bound methyl groups.

In **2** and **2′** the metal atom is located 1.615 and 1.608 Å above the C_2B_3 carborane faces, respectively. The planes defined by the metal-bonded atoms of the Cp* ligand are inclined by 6.3° and 8.3°, respectively, to the metal-bonded C_2B_3 faces, and, as was the case with compound **1**, the Cp* methyl groups nearest to the SMe_2 substituent suffer the greatest out-of-plane distortion, C(44) lying 0.286 and C(41′) 0.252 Å above the η^5-C_5 ring, 1.862 and 1.842 Å below which sit Ru(3) and Ru(3′).

If a $CDCl_3$ solution of compound **2** is left at room temperature for 5 days (or gently heated to reflux for ca. 1 h), peaks in the ^{1}H NMR spectrum due to **2** disappear and are replaced cleanly by new signals. The aromatic region of the spectrum no longer shows the broad, intensity two, signal indicative of a phenyl group undergoing restricted rotation. Instead, two sharp multiplets centered on 7.36 and 7.07 ppm, of intensity 2 and 3, respectively, are observed, suggesting that in this new compound phenyl rotation is unrestricted. New signals due to cage C−H, SMe_2, and Cp* are also observed in the same relative ratios as in compound **2**, suggesting isomerization has occurred. The ^{11}B{^{1}H} NMR spectrum of the new compound, **3**, reveals eight peaks between 1.3 and −24.0 ppm, although we could not determine which was due to B bound to S; $\langle\delta(^{11}B)\rangle = -10.31$ ppm, implying that **3** also has a *closo*-RuC_2B_9 cage architecture. This was ultimately confirmed by a crystallographic study, which revealed that compound **3** is 3-(Cp*)-4-SMe_2-11-Ph-3,1,2-*closo*-$RuC_2B_9H_{10}$. A perspective view of a single molecule, demonstrating the atom-numbering scheme used, is shown in Figure 4, and selected bond distances and interbond angles are listed in Table 4.

The C−Ph group of **3** has moved from the upper to the lower pentagonal belt of the molecule relative to the precursor **2**, and the C−C connectivity has been broken. The SMe_2 group remains in the upper belt, now CB_4, adjacent to the cage C atom, and the conformation of the SMe_2 unit is defined by a τ value of −28.4°. Since a CB_4 pentagon is somewhat larger than a C_2B_3 one, Ru(3) is required to lie closer to the carborane ligand

Table 3. Selected Bond Lengths (Å) and Angles (deg) in Compound 2

Ru(3)−C(1)	2.175(10)	Ru(3)−C(2)	2.173(9)	Ru(3)−C(35)	2.177(11)
Ru(3)−B(7)	2.180(10)	Ru(3)−B(4)	2.197(12)	Ru(3)−C(31)	2.200(10)
Ru(3)−B(8)	2.225(12)	Ru(3)−C(32)	2.229(10)	Ru(3)−C(34)	2.231(11)
Ru(3)−C(33)	2.253(11)	S(1)−C(21)	1.791(14)	S(1)−C(20)	1.794(12)
S(1)−B(7)	1.927(14)	C(1)−C(11)	1.510(14)	C(1)−C(2)	1.669(13)
C(1)−B(5)	1.695(14)	C(1)−B(4)	1.718(14)	C(1)−B(6)	1.75(2)
C(2)−B(11)	1.70(2)	C(2)−B(7)	1.70(2)	C(2)−B(6)	1.750(14)
B(4)−B(9)	1.78(2)	B(4)−B(5)	1.78(2)	B(4)−B(8)	1.80(2)
B(5)−B(6)	1.72(2)	B(5)−B(9)	1.76(2)	B(5)−B(10)	1.77(2)
B(6)−B(11)	1.76(2)	B(6)−B(10)	1.78(2)	B(7)−B(12)	1.77(2)
B(7)−B(11)	1.78(2)	B(7)−B(8)	1.80(2)	B(8)−B(9)	1.79(2)
B(8)−B(12)	1.84(2)	B(9)−B(12)	1.77(2)	B(9)−B(10)	1.79(2)
B(10)−B(12)	1.77(2)	B(10)−B(11)	1.78(2)	B(11)−B(12)	1.79(2)
Ru(3′)−B(7′)	2.150(12)	Ru(3′)−C(32′)	2.162(12)	Ru(3′)−C(2′)	2.171(11)
Ru(3′)−C(33′)	2.183(12)	Ru(3′)−C(1′)	2.196(11)	Ru(3′)−C(34′)	2.202(12)
Ru(3′)−B(8′)	2.200(12)	Ru(3′)−B(4′)	2.212(13)	Ru(3′)−C(35′)	2.216(13)
Ru(3′)−C(31′)	2.233(12)	S(1′)−C(21′)	1.742(12)	S(1′)−C(20′)	1.810(12)
S(1′)−B(7′)	1.920(13)	C(1′)−C(11′)	1.50(2)	C(1′)−C(2′)	1.66(2)
C(1′)−B(5′)	1.72(2)	C(1′)−B(6′)	1.74(2)	C(1′)−B(4′)	1.74(2)
C(2′)−B(7′)	1.72(2)	C(2′)−B(11′)	1.71(2)	C(2′)−B(6′)	1.74(2)
B(4′)−B(9′)	1.77(2)	B(4′)−B(5′)	1.78(2)	B(4′)−B(8′)	1.80(2)
B(5′)−B(9′)	1.75(2)	B(5′)−B(10′)	1.77(2)	B(5′)−B(6′)	1.79(2)
B(6′)−B(11′)	1.71(2)	B(6′)−B(10′)	1.75(2)	B(7′)−B(12′)	1.77(2)
B(7′)−B(8′)	1.77(2)	B(7′)−B(11′)	1.79(2)	B(8′)−B(9′)	1.80(2)
B(8′)−B(12′)	1.80(2)	B(9′)−B(10′)	1.76(2)	B(9′)−B(12′)	1.76(2)
B(10′)−B(11′)	1.77(2)	B(10′)−B(12′)	1.80(2)	B(11′)−B(12′)	1.79(2)
C(1)−Ru(3)−C(2)	45.2(3)	C(1)−Ru(3)−B(7)	78.4(4)	C(2)−Ru(3)−B(7)	46.1(4)
C(1)−Ru(3)−B(4)	46.3(4)	C(2)−Ru(3)−B(4)	79.2(4)	B(7)−Ru(3)−B(4)	80.9(5)
C(1)−Ru(3)−B(8)	80.3(4)	C(2)−Ru(3)−B(8)	80.7(4)	B(7)−Ru(3)−B(8)	48.2(4)
B(4)−Ru(3)−B(8)	48.1(4)	C(35)−Ru(3)−C(32)	62.3(4)	C(31)−Ru(3)−C(32)	36.3(4)
C(35)−Ru(3)−C(34)	38.0(4)	C(31)−Ru(3)−C(34)	62.4(4)	C(32)−Ru(3)−C(34)	62.6(4)
C(35)−Ru(3)−C(33)	62.2(4)	C(31)−Ru(3)−C(33)	61.1(4)	C(32)−Ru(3)−C(33)	37.1(4)
C(34)−Ru(3)−C(33)	37.1(4)	C(21)−S(1)−C(20)	99.6(6)	C(21)−S(1)−B(7)	109.6(6)
C(20)−S(1)−B(7)	100.1(5)				
B(7′)−Ru(3′)−C(2′)	46.9(5)	C(32′)−Ru(3′)−C(33′)	37.4(5)	B(7′)−Ru(3′)−C(1′)	78.6(4)
C(2′)−Ru(3′)−C(1′)	44.8(4)	C(33′)−Ru(3′)−C(1′)	128.6(5)	C(32′)−Ru(3′)−C(34′)	62.4(5)
C(33′)−Ru(3′)−C(34′)	38.3(5)	B(7′)−Ru(3′)−B(8′)	48.1(5)	C(2′)−Ru(3′)−B(8′)	81.0(5)
B(7′)−Ru(3′)−B(4′)	81.3(5)	C(2′)−Ru(3′)−B(4′)	79.5(5)	C(1′)−Ru(3′)−B(4′)	46.4(4)
B(8′)−Ru(3′)−B(4′)	48.3(5)	C(32′)−Ru(3′)−C(35′)	62.2(5)	C(33′)−Ru(3′)−C(35′)	63.2(5)
C(34′)−Ru(3′)−C(35′)	37.1(5)	C(32′)−Ru(3′)−C(31′)	37.1(5)	C(33′)−Ru(3′)−C(31′)	62.9(5)
C(34′)−Ru(3′)−C(31′)	62.1(5)	C(35′)−Ru(3′)−C(31′)	37.3(5)	C(21′)−S(1′)−C(20′)	102.7(6)
C(21′)−S(1′)−B(7′)	105.1(6)	C(20′)−S(1′)−B(7′)	107.6(6)		

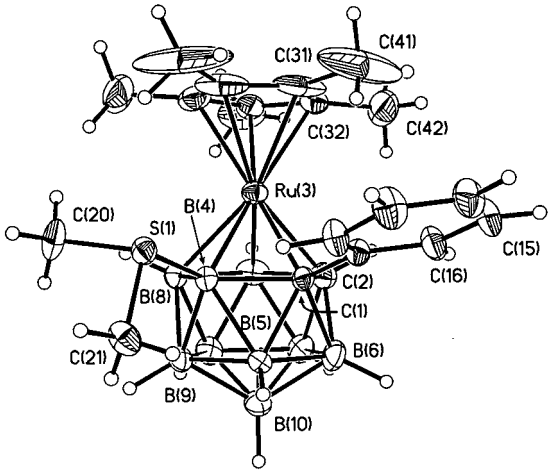

Figure 4. Perspective view of compound **3**, with thermal ellipsoids and H atoms drawn as in Figure 1.

face,[19] being only 1.547 Å above the CB_4 least-squares plane. Intramolecular crowding is apparent from a 9.1° tilt of the η^5-C_5 plane relative to the carborane CB_4 plane, with the side of the Cp* ligand near the SMe_2 substituent [C(35)−C(45)] displaced upward. Since the Ru···CB_4 plane distance in **3** is short, the Ru···C_5 plane distance is relatively long, 1.872 Å.

In a manner similar to that which afforded **1** and **2**, carborane **IIb** was deprotonated (NaH) and reacted with $[RuCl(Cp^*)]_4$ to afford 1-Ph-3-(Cp*)-4-SMe_2-3,1,2-$RuC_2B_9H_{10}$, **4**, in moderate yield after workup by column chromatography. Expecting this compound to be more sterically crowded than **2**, since the SMe_2 and Ph substituents are now on adjacent cage atoms, we characterized **4** by single-crystal *X*-ray analysis as well as by multinuclear NMR spectroscopy. Compound **4** crystallizes with no close intermolecular contacts, and a perspective diagram showing the atom-numbering scheme is given in Figure 5, while key molecular parameters are listed in Table 5.

Although there is some evidence of contact between the SMe_2 and phenyl groups in **4**, it clearly does not dramatically deform the structure. Thus, C(2)−B(4), 1.743(8) Å, is longer than the equivalent distances in **1**, **2**, and **2′** (1.70(2)−1.72(2) Å) and the angle S(1)−B(4)−C(1) is similarly wider, 123.7(4)° versus 119.1(3)−120.3(7)°. C(1)−C(2), 1.713(9) Å, is also greater in **4** than in the aforementioned analogues. In **4**, τ is −38.4° and the conformation of the phenyl substituent is specified by a θ value (θ is the modulus of the average $C_{phenyl}-C_{phenyl}-C_{cage}-C_{cage}$ torsion angle[13b]) of 73.9°. Ru(3) sits 1.578 Å above the carborane C_2B_3 face and 1.853 Å below the η^5-C_5 face, with an interfacial angle

(19) Elian, M.; Chen, M. M. L.; Mingos, D. M. P.; Hoffmann, R. *Inorg. Chem.* **1976**, *15*, 1148.

Table 4. Selected Bond Lengths (Å) and Angles (deg) in Compound 3

Ru(3)−B(4)	2.133(9)	Ru(3)−B(2)	2.143(9)	Ru(3)−B(7)	2.154(11)
Ru(3)−C(1)	2.181(9)	Ru(3)−C(32)	2.204(9)	Ru(3)−B(8)	2.209(10)
Ru(3)−C(31)	2.213(10)	Ru(3)−C(33)	2.242(7)	Ru(3)−C(34)	2.251(7)
Ru(3)−C(35)	2.254(9)	S(1)−C(21)	1.782(12)	S(1)−C(20)	1.793(9)
S(1)−B(4)	1.935(9)	C(1)−B(6)	1.717(13)	C(1)−B(2)	1.756(13)
C(1)−B(4)	1.770(13)	C(1)−B(5)	1.776(14)	B(2)−C(11)	1.773(13)
B(2)−B(6)	1.794(13)	B(2)−B(7)	1.844(14)	B(4)−B(8)	1.738(14)
B(4)−B(9)	1.763(14)	B(4)−B(5)	1.771(12)	B(5)−B(9)	1.74(2)
B(5)−B(10)	1.75(2)	B(5)−B(6)	1.767(14)	B(6)−C(11)	1.730(13)
B(6)−B(10)	1.79(2)	B(7)−C(11)	1.771(12)	B(7)−B(8)	1.785(13)
B(7)−B(12)	1.83(2)	B(8)−B(12)	1.752(14)	B(8)−B(9)	1.76(2)
B(9)−B(10)	1.732(14)	B(9)−B(12)	1.76(2)	B(10)−C(11)	1.725(12)
B(10)−B(12)	1.75(2)	C(11)−C(111)	1.498(12)	C(11)−B(12)	1.724(13)
B(4)−Ru(3)−B(2)	83.2(3)	B(4)−Ru(3)−B(7)	82.8(4)	B(2)−Ru(3)−B(7)	50.8(4)
B(4)−Ru(3)−C(1)	48.4(3)	B(2)−Ru(3)−C(1)	47.9(3)	B(7)−Ru(3)−C(1)	84.1(4)
B(4)−Ru(3)−B(8)	47.1(4)	B(2)−Ru(3)−B(8)	84.1(4)	B(7)−Ru(3)−B(8)	48.3(4)
C(1)−Ru(3)−B(8)	82.4(4)	C(32)−Ru(3)−C(31)	37.3(4)	C(32)−Ru(3)−C(33)	37.5(5)
C(32)−Ru(3)−C(34)	63.1(4)	C(31)−Ru(3)−C(34)	62.3(4)	C(33)−Ru(3)−C(34)	37.6(3)
C(32)−Ru(3)−C(35)	62.5(3)	C(31)−Ru(3)−C(35)	37.0(3)	C(33)−Ru(3)−C(35)	62.2(5)
C(34)−Ru(3)−C(35)	37.3(4)	C(21)−S(1)−C(20)	98.4(6)	C(21)−S(1)−B(4)	101.4(5)
C(20)−S(1)−B(4)	109.2(4)				

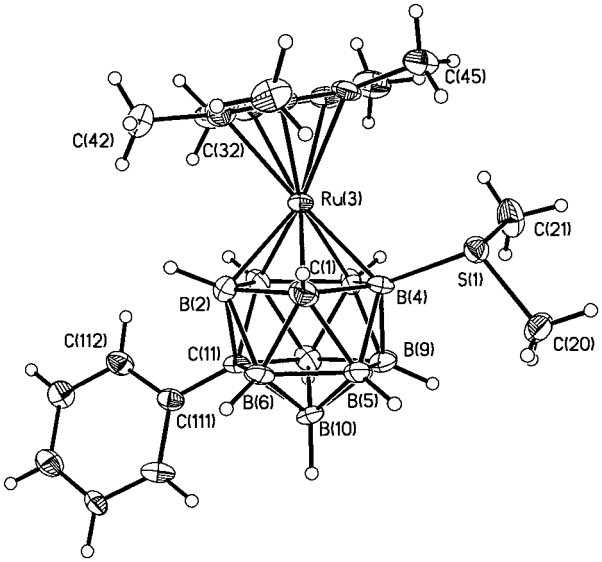

Figure 5. Perspective view of compound **4**, with thermal ellipsoids and H atoms drawn as in Figure 1.

of 8.3°. Distances within the 12-vertex cluster are unexceptional.

The ^{1}H NMR spectrum of compound **4** displays Cp* and SMe_2 methyl resonances at the expected frequencies. The C_{cage}−H signal is observed at 3.18 ppm, ca. 0.8 ppm to lower frequency and ca. 1.0 ppm to higher frequency than in the isomeric compounds **2** and **3**. Three sharp signals, in the ratio 2:1:2, are observed for the phenyl protons, implying free rotation of this group on the NMR time scale (contrast with compound **2**). The ^{11}B{^{1}H} NMR spectrum displays seven resonances between 0.8 and −20.3 ppm ($<\delta(^{11}B)> = -10.36$ ppm), in the ratio (high frequency to low frequency) 1:1:2:1:1:2:1, with that at 0.05 ppm assigned to B(7). Unlike **2**, compound **4** shows no tendency to undergo low-temperature polytopal isomerization. Heating a $CDCl_3$ solution of **4** to reflux only resulted (^{1}H NMR) in unchanged **4** along with small amounts of unidentified decomposition products; heating a toluene solution of compound **4** to reflux caused complete decomposition.

Deprotonation of the trisubstituted carborane **III** and subsequent reaction with $[RuCl(Cp^*)]_4$ affords 1,2-Ph_2-3-(Cp*)-4-SMe_2-3,1,2-*pseudocloso*-$RuC_2B_9H_9$, **5**, in modest yield. Compound **5** was initially characterized by ^{1}H and ^{11}B{^{1}H} NMR spectroscopy and ultimately by a single-crystal *X*-ray diffraction study. The ^{1}H NMR spectrum is relatively uninformative, showing resonances due to the phenyl and inequivalent SMe groups in the expected positions. The ^{11}B{^{1}H} spectrum displays eight resonances in the range from 27.2 to −16.4 ppm, in the ratio (high to low frequency) 1:1:1:1:1:2:1:1. Not only is this a significantly larger chemical shift range than that found for the closo compounds **1**−**4**, but also the average shift, $<\delta(^{11}B)>$, is +2.60 ppm, substantially to higher frequency and characteristic of a pseudocloso structure.[2,18,20−22] Note that although $<\delta(^{11}B)>$ for **5** lies ca. 3−4 ppm to lower frequency than that previously reported for pseudocloso (η^6-arene)-$RuPh_2C_2B_9H_9$ compounds, the difference can be fully accounted for by correcting for the differences in polyene and carborane, since, typically, $<\delta(^{11}B)>$ for **1** is −12.6 ppm while $<\delta(^{11}B)>$ for 1-Ph-3-(cym)-3,1,2-*closo*-$RuC_2B_9H_{10}$ is −8.0 ppm.[13b] In **5**, the ^{11}B resonance at −1.63 ppm is assigned to B(4).

Figure 6 shows a perspective view of compound **5**, and Table 6 gives selected molecular parameters. It is immediately apparent that **5** adopts the pseudocloso structure implied by the NMR results, steric pressure from the Cp* ligand forcing the adjacent phenyl groups to adopt high θ values (74.7° and 78.3°) and, thus, push against each other, stretching the C(1)−C(2) connectivity to 2.533(11) Å. Previously, we have described pseudocloso compounds derived from the [7,8-Ph_2-7,8-*nido*-$C_2B_9H_9$]$^{2-}$ ligand with capping metal fragments such as {Ru(η^6arene)},[2,21] {Ru(κ^3-$S_3C_6H_{12}$)},[22] and {Rh(Cp*)}.[20] Compound **5**, the first pseudocloso charge-compensated carbametallaborane, is fully analogous to all of these. The conformation of the SMe_2 group is described by $\tau = -41.5°$. Ru(3) lies 1.451 Å above the carborane C_2B_3 plane and 1.894 Å below the η^5-C_5 plane,

(20) Lewis, Z. G.; Welch, A. J. *J. Organomet. Chem.* **1992**, *430*, C45.
(21) Brain, P. T.; Bühl, M.; Cowie, J.; Lewis, Z. G.; Welch, A. J. *J. Chem. Soc., Dalton Trans.* **1996**, 231.
(22) Weller, A. S.; Welch, A. J. *Inorg. Chem.* **1996**, *35*, 4538.

Table 5. Selected Bond Lengths (Å) and Angles (deg) in Compound 4

Ru(3)−C(2)	2.118(6)	Ru(3)−C(1)	2.155(5)	Ru(3)−B(4)	2.166(7)
Ru(3)−C(34)	2.180(7)	Ru(3)−C(33)	2.181(5)	Ru(3)−B(7)	2.185(9)
Ru(3)−C(32)	2.202(7)	Ru(3)−C(35)	2.220(8)	Ru(3)−B(8)	2.222(7)
Ru(3)−C(31)	2.236(8)	S(1)−C(20)	1.798(6)	S(1)−C(21)	1.799(7)
S(1)−B(4)	1.924(8)	C(1)−C(11)	1.505(8)	C(1)−B(5)	1.712(7)
C(1)−C(2)	1.713(9)	C(1)−B(4)	1.743(8)	C(1)−B(6)	1.754(9)
C(2)−B(11)	1.702(11)	C(2)−B(7)	1.710(11)	C(2)−B(6)	1.731(10)
B(4)−B(9)	1.766(10)	B(4)−B(8)	1.792(10)	B(4)−B(5)	1.799(9)
B(5)−B(6)	1.728(11)	B(5)−B(10)	1.749(11)	B(5)−B(9)	1.768(9)
B(6)−B(10)	1.751(11)	B(6)−B(11)	1.768(13)	B(7)−B(12)	1.774(10)
B(7)−B(11)	1.790(11)	B(7)−B(8)	1.792(12)	B(8)−B(12)	1.781(11)
B(8)−B(9)	1.794(9)	B(9)−B(10)	1.753(10)	B(9)−B(12)	1.756(13)
B(10)−B(11)	1.756(11)	B(10)−B(12)	1.763(11)	B(11)−B(12)	1.774(11)
C(2)−Ru(3)−C(1)	47.3(2)	C(2)−Ru(3)−B(4)	80.2(3)	C(1)−Ru(3)−B(4)	47.6(2)
C(34)−Ru(3)−C(33)	37.1(3)	C(2)−Ru(3)−B(7)	46.8(3)	C(1)−Ru(3)−B(7)	82.3(3)
B(4)−Ru(3)−B(7)	82.3(3)	C(33)−Ru(3)−B(7)	96.3(3)	C(34)−Ru(3)−C(32)	62.6(3)
C(33)−Ru(3)−C(32)	37.1(3)	C(2)−Ru(3)−C(35)	156.7(5)	C(34)−Ru(3)−C(35)	36.6(4)
C(33)−Ru(3)−C(35)	61.5(3)	C(32)−Ru(3)−C(35)	62.7(4)	C(2)−Ru(3)−B(8)	80.2(3)
C(1)−Ru(3)−B(8)	82.2(2)	B(4)−Ru(3)−B(8)	48.2(3)	B(7)−Ru(3)−B(8)	48.0(3)
C(34)−Ru(3)−C(31)	61.5(4)	C(33)−Ru(3)−C(31)	61.3(3)	C(32)−Ru(3)−C(31)	37.4(4)
C(35)−Ru(3)−C(31)	37.1(4)	C(20)−S(1)−C(21)	100.1(3)	C(20)−S(1)−B(4)	101.8(4)
C(21)−S(1)−B(4)	107.1(3)				

Table 6. Selected Bond Lengths (Å) and Angles (deg) in Compound 5

Ru(3)−C(1)	2.147(7)	Ru(3)−C(2)	2.159(7)	Ru(3)−B(4)	2.174(9)
Ru(3)−C(33)	2.193(8)	Ru(3)−B(7)	2.196(8)	Ru(3)−C(34)	2.202(8)
Ru(3)−B(8)	2.210(10)	Ru(3)−C(32)	2.254(9)	Ru(3)−C(35)	2.263(9)
Ru(3)−C(31)	2.290(8)	S(1)−C(51)	1.790(9)	S(1)−C(52)	1.809(9)
S(1)−B(4)	1.933(9)	C(1)−C(11)	1.504(10)	C(1)−B(5)	1.634(11)
C(1)−B(4)	1.648(11)	C(1)−B(6)	1.743(11)	C(2)−C(21)	1.495(11)
C(2)−B(11)	1.631(11)	C(2)−B(7)	1.654(13)	C(2)−B(6)	1.758(11)
B(7)−B(8)	1.763(12)	B(7)−B(12)	1.807(12)	B(7)−B(11)	1.857(14)
B(11)−B(10)	1.725(14)	B(11)−B(12)	1.770(14)	B(11)−B(6)	1.829(12)
B(6)−B(5)	1.799(12)	B(6)−B(10)	1.886(12)	B(4)−B(9)	1.798(13)
B(4)−B(8)	1.811(12)	B(4)−B(5)	1.824(12)	B(8)−B(12)	1.763(13)
B(8)−B(9)	1.798(13)	B(12)−B(9)	1.741(13)	B(12)−B(10)	1.769(14)
B(10)−B(5)	1.756(13)	B(10)−B(9)	1.759(13)	B(5)−B(9)	1.802(13)
C(1)−Ru(3)−C(2)	72.1(3)	C(1)−Ru(3)−B(4)	44.9(3)	C(2)−Ru(3)−B(4)	94.8(3)
C(1)−Ru(3)−B(7)	96.4(3)	C(2)−Ru(3)−B(7)	44.6(4)	B(4)−Ru(3)−B(7)	86.7(3)
C(33)−Ru(3)−C(34)	37.6(4)	C(1)−Ru(3)−B(8)	84.2(3)	C(2)−Ru(3)−B(8)	82.1(3)
B(4)−Ru(3)−B(8)	48.8(3)	B(7)−Ru(3)−B(8)	47.2(3)	C(33)−Ru(3)−C(32)	36.4(4)
C(34)−Ru(3)−C(32)	60.9(3)	C(33)−Ru(3)−C(35)	61.9(3)	C(34)−Ru(3)−C(35)	37.0(3)
C(32)−Ru(3)−C(35)	60.4(3)	C(33)−Ru(3)−C(31)	60.5(3)	C(34)−Ru(3)−C(31)	60.3(3)
C(32)−Ru(3)−C(31)	35.7(4)	C(35)−Ru(3)−C(31)	35.7(3)	C(51)−S(1)−C(52)	99.2(5)
C(51)−S(1)−B(4)	103.2(4)	C(52)−S(1)−B(4)	107.2(4)		

and the two planes are inclined (6.0°) such that the Cp* ligand tilts away from the SMe_2 unit.

Conclusions

We have demonstrated that $[Ru(Cp^*)Cl]_4$ is a versatile reagent for the incorporation of {Ru(Cp*)} fragments into carborane cages. Using this robust synthon, we have isolated examples of sterically encumbered charge-compensated carboranes, including three isomers of $Cp^*RuPh(SMe_2)C_2B_9H_9$ (compounds **2**−**4**). Somewhat unexpectedly, the compound in which the phenyl and SMe_2 groups are separated by one cage carbon atom (compound **2**) displays restricted rotation of the Ph substituent at room temperature and undergoes relatively facile polyhedral isomerization while that in which Ph and SMe_2 are adjacent (compound **4**) has a freely rotating Ph group at room temperature in solution and shows no tendency to rearrange, even on gentle thermolysis. A possible explanation, at least for the Ph rotation, could be that in **4** the Cp* cap tilts out of the way of a spinning phenyl group whereas similar tilting in **2** would be prohibited. The first example of a charge-compensated pseudocloso metallacarborane (compound **5**) is also reported.

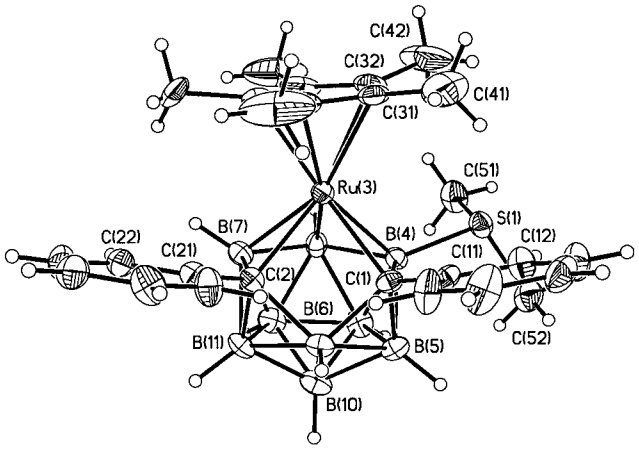

Figure 6. Perspective view of compound **5**, with thermal ellipsoids and H atoms drawn as in Figure 1.

The ability to label boron atoms in sterically crowded metallaboranes affords the possibility of following the movement of specific boron atoms in polyhedral re-

arrangements, and studies are currently underway[23] using carborane fragments such as **III** in systems that have been shown to isomerize at low temperatures via isolatable intermediates.[4]

Acknowledgment. We thank Callery Chemical Co. for their generous gift of chemicals and the Engineering and Physical Sciences Research Council for provision of postdoctoral fellowships to G.M.R. and A.S.W.

(23) Dunn, S.; Rosair, G. M.; Weller, A. S.; Welch, A. J. *J. Chem. Soc., Chem. Commun.* **1998**, 1065, and work in progress.

Supporting Information Available: Tables of atomic coordinates, thermal parameters, and bond lengths and angles (51 pages). Ordering information is given on any current masthead page.

OM980353V